

Article

Enhanced Emission by Accumulated Charges at Organic/Metal Interfaces Generated during the Reverse Bias of Organic Light Emitting Diodes

Soichiro Nozoe and Masaki Matsuda * 

Department of Chemistry, Kumamoto University, Kumamoto, Kumamoto 860-8555, Japan; nze.225@gmail.com

* Correspondence: masaki@kumamoto-u.ac.jp; Tel.: +81-96-342-3372

Received: 13 September 2017; Accepted: 9 October 2017; Published: 12 October 2017

Abstract: A high frequency rectangular alternating voltage was applied to organic light emitting diodes (OLEDs) with the structure ITO/TPD/Alq₃/Al and ITO/CoPc/Alq₃/Al, where ITO is indium-tin-oxide, TPD is 4,4'-bis[N-phenyl-N-(m-tolyl)amino]biphenyl, CoPc is cobalt phthalocyanine, and Alq₃ is Tris(8-quinolinolato)aluminum, and the effect on emission of the reverse bias was examined. The results reveal that the emission intensity under an alternating reverse-forward bias is greater than that under an alternating zero-forward bias. The difference in the emission intensity (ΔI) increased both for decreasing frequency and increasing voltage level of the reverse bias. In particular, the change in emission intensity was proportional to the voltage level of the reverse bias given the same frequency. To understand ΔI , this paper proposes a model in which an OLED works as a capacitor under reverse bias, where positive and negative charges accumulate on the metal/organic interfaces. In this model, the emission enhancement that occurs during the alternating reverse-forward bias is rationalized as a result of the charge accumulation at the organic/metal interfaces during the reverse bias, which possibly modulates the vacuum level shifts at the organic/metal interfaces to reduce both the hole injection barrier at the organic/ITO interface and the electron injection barrier at the organic/Al interface under forward bias.

Keywords: organic light emitting diode; reverse-bias application; charge accumulation; emission enhancement

1. Introduction

About 25 years after the first report of electroluminescence from a single crystal of anthracene under a high applied voltage [1], Tang proposed an organic light emitting diode (OLED) composed of a double-layer structure of organic thin films [2]. Since then, various OLEDs with different structures have been developed. The device structures are designed based on the work functions of the electrodes and molecular orbital energy levels of the organic materials, which are key factors of the OLEDs' performance. Meanwhile, using ultraviolet photoemission spectroscopy and the Kelvin probe method, Ishii et al. discovered the vacuum level shift at various organic/metal interfaces, where band bending does not occur [3,4], meaning that the Mott-Schottky model is not applicable to OLEDs. Furthermore, by using a time-resolved optical second harmonic generation measurement while applying a rectangular alternating voltage to typical OLEDs, Iwamoto et al. reported that charges accumulate at the organic/organic interface under forward bias with high frequency, and they proposed a model of emission induced by the accumulated charges at the organic/organic interface [5–8]. Moreover, these studies signify that, to understand the OLED emission mechanism and control its performance, we must focus on the electronic states at the interfaces as well as the work functions and molecular orbital energy levels.

We have been attracted by the report that the emission intensity for an ITO/ α -NPD/Alq₃/Al device under an alternating reverse-forward bias becomes higher than that under an alternating zero-forward bias in the frequency region between 8×10^5 and 10 Hz [7]. The change in the emission intensity is reported to be due to suppression of the charge injection caused by the charge accumulation at the organic/organic interface under the alternating zero-forward bias.

In this study, we focused on the effect of reverse bias on the device properties. Zou et al. reported that a reverse bias with a long application time (10^1 – 10^4 s) induces the movement of ionic impurities in the active layer, leading to emission enhancement and lifetime improvement [9,10]; however, this mechanism is not acceptable in the high frequency region because the ionic impurities could not follow the frequency. To investigate the generality of the higher emission intensity under an alternating reverse-forward bias than that under an alternating zero-forward bias, OLEDs with the structure ITO/TPD/Alq₃/Al and ITO/CoPc/Alq₃/Al were fabricated, where TPD is 4,4'-bis[N-phenyl-N-(m-tolyl)amino]biphenyl, Alq₃ is Tris(8-quinolinolato)aluminum, and CoPc is cobalt phthalocyanine. We propose another model in which an OLED works as a capacitor under reverse bias, and the accumulated charges at the organic/metal interfaces induce an enhancement of emission under the alternating reverse-forward bias.

2. Materials and Methods

CoPc was synthesized following the procedure reported in [11], and used as a hole injection and transport material. TPD was used as a hole injection and transport material and Alq₃ was used as an electron injection, transport, and emitting material. Both are commercially available from Tokyo Kasei and were used without further purification.

The OLEDs were fabricated by the vacuum deposition of TPD or CoPc and Alq₃ films (30 nm), followed by the Al cathode (30 nm) on an ITO (indium-tin-oxide) electrode. The base pressure for the organic materials and Al was less than 1.5×10^{-5} torr and 5.0×10^{-6} torr, respectively. The ITO substrate was cleaned by ultrasonic agitation for 15 min in acetone, 2-propanol, and methanol prior to film fabrications. Energy diagrams of the fabricated devices are shown in Figure 1.

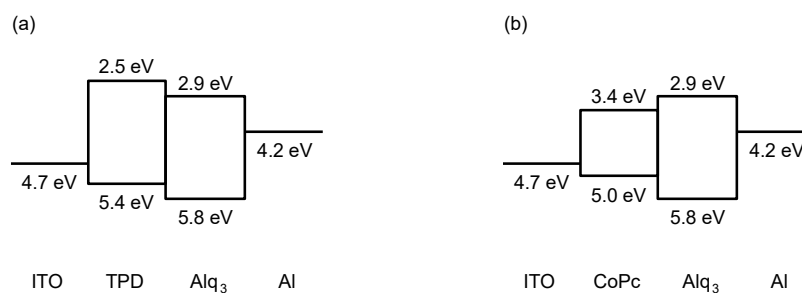


Figure 1. Energy diagram of the ITO/TPD/Alq₃/Al device (a) and ITO/CoPc/Alq₃/Al device (b). The energy levels of organic materials and electrodes are cited from [12].

An alternating rectangular voltage of various frequencies was applied using a Keithley 3390 waveform generator. The duty ratio for the applied alternating rectangular voltage signal was always 50%. The emission spectra were measured using an Ocean Optics QE65000 spectrometer with a 10 s exposure time. All measurements were performed in a vacuum (less than 1.0×10^{-4} torr) in an Oxford Optistat-CF cryostat.

Because of the deterioration of the devices, the measurements of the frequency dependence (Figure 2) and reverse-bias voltage dependence (Figure 3) were performed using different devices. However, the reproducibility of the tendency of the emission properties was ascertained several times using several devices for each measurement.

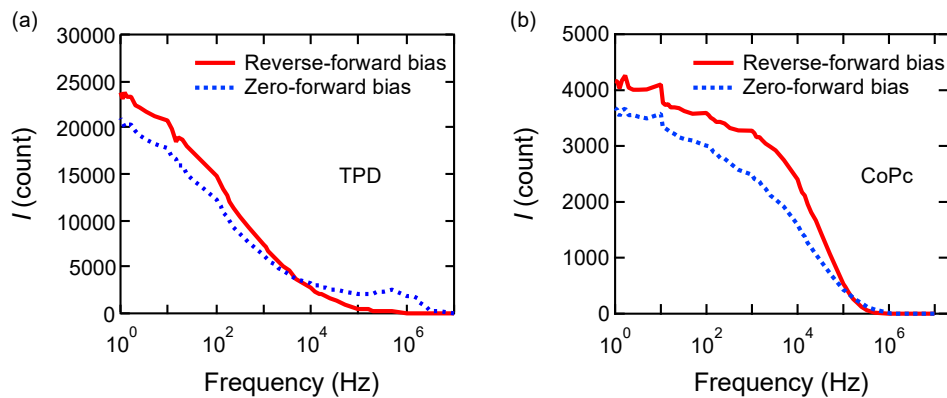


Figure 2. Emission intensity I versus the frequency f of the voltage for the ITO/TPD/Alq₃/Al device (a) and ITO/CoPc/Alq₃/Al device (b). The solid and dashed lines indicate the emission intensity under -10 and 10 V (reverse-forward) bias and 0 and 10 V (zero-forward) bias, respectively.

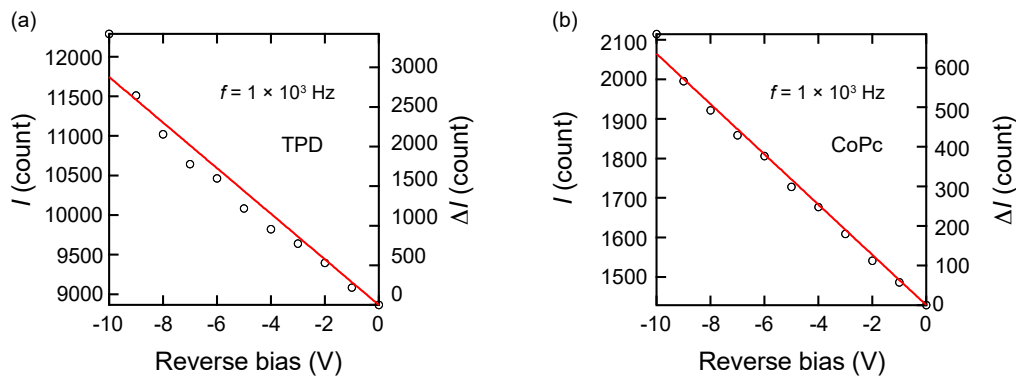


Figure 3. I (left axis) and ΔI (right axis) versus applied reverse-bias voltage alternated with forward 10 V with 1×10^3 Hz for the ITO/TPD/Alq₃/Al device (a) and ITO/CoPc/Alq₃/Al device (b). The solid line is ΔI calculated using Equation (6) (see main text).

3. Results and Discussion

Figure 2 shows the emission intensity (I) as a function of the frequency (f), which alternated between -10 and 10 V (for reverse-forward bias) and 0 and 10 V (for zero-forward bias). In both devices, I decreased when the frequency increased under both reverse-forward and zero-forward biases. Under the reverse-forward bias, I is higher than under the zero-forward bias in the frequency region between 1 and 5×10^3 Hz and 1 and 1×10^5 Hz for the ITO/TPD/Alq₃/Al and ITO/CoPc/Alq₃/Al devices, respectively. These results resemble that reported in [7], suggesting that the higher emission intensity under an alternating reverse-forward bias than under an alternating zero-forward bias is generally observed in OLEDs.

We investigated how the reverse-bias voltage alters I . Figure 3 depicts I as a function of the reverse-bias voltage alternated with a 10 V forward bias with $f = 1 \times 10^3$ Hz. In this figure, I linearly correlates with the reverse-bias voltage. Because the change in emission intensity (ΔI) can be regarded as the difference of I under zero-forward bias and that under reverse-forward bias, ΔI is also proportional to the applied reverse-bias voltage, as shown on the right axis of Figure 3. This result signifies that ΔI depends on both the frequency and applied voltage of the reverse bias.

In [7], ΔI is rationalized by a model in which excess charges accumulate at the organic/organic interface: the accumulated charges under the alternating zero-forward bias suppress the charge injection, and induce the decrease in the emission intensity. The model is reasonable, however, the proportional dependence of the emission intensity change on the reverse-bias voltage, observed in this study is unclear in the model. Here, we focus on the proportional dependence, and propose another

model in which an OLED acts as a capacitor during the reverse bias, where positive and negative charges respectively accumulate on the organic/Al and organic/ITO interfaces, and the accumulated charges at the organic/metal interfaces induce an enhancement of emission under the alternating reverse-forward bias. A series circuit of two parallel circuits of a resistor and capacitor is described to understand the charge accumulation at the organic/organic interface in a double-layer OLED [7,13]. In contrast, to estimate the charge accumulation at the organic/metal interfaces, the equivalent circuit shown in Figure 4, which is a series circuit of a resistor and a parallel circuit of a resistor and capacitor, is considered. The circuit equations are as follows

$$V = R_1 i_{R_1} + \frac{1}{C} \int i_c dt$$

$$i_{R_1} = i_{R_2} + i_c$$

$$R_2 i_{R_2} = \frac{1}{C} \int i_c dt$$

where V is the absolute value of the applied reverse-bias voltage, i is current, C is capacitance, R_1 is the internal resistance, R_2 is the resistance of the OLED, and t is the time of the reverse-bias application, which is half the reciprocal of the frequency ($t = \frac{1}{2}f^{-1}$). These equations lead to the equation

$$R_2 \frac{1}{R_1 + R_2} (V - R_1 i_c) = \frac{1}{C} \int i_c dt. \quad (1)$$

Because i_c can be denoted as $i_c = dQ_c/dt$ using the quantity of electric charge (Q_c), Equation (1) can be expressed as

$$R_2 \frac{1}{R_1 + R_2} \left(V - R_1 \frac{dQ_c}{dt} \right) = \frac{1}{C} Q_c, \quad (2)$$

which can be transformed into

$$\frac{dQ_c}{dt} + \frac{R_1 + R_2}{R_1 R_2 C} Q_c = \frac{V}{R_1}. \quad (3)$$

Considering an initial condition of $Q_c = 0$, Equation (3) can be solved as

$$Q_c = \frac{R_2}{R_1 + R_2} CV \left\{ 1 - \exp \left(- \frac{R_1 + R_2}{R_1 R_2 C} t \right) \right\}, \quad (4)$$

and supposing the emission intensity change induced by the accumulated charges (ΔI_a) is proportional to Q_c , we obtain

$$\Delta I_a = \frac{R_2}{R_1 + R_2} ACV \left\{ 1 - \exp \left(- \frac{R_1 + R_2}{R_1 R_2 C} t \right) \right\}. \quad (5)$$

by introducing proportionality constant A . Here, because ΔI_a is the change in emission intensity during t , ΔI for an exposure time of 10 s can be denoted as

$$\Delta I = \frac{5}{t} \Delta I_a. \quad (6)$$

This equation adequately reproduces the observed proportional dependence of the emission intensity change on the reverse-bias voltage. With the parameter sets $R_1 = 50 \Omega$, $R_2 = 5.0 \times 10^6 \Omega$, and $C = 10 \times 10^{-9} \text{ F}$, where R_1 and R_2 are the estimated resistances of the ITO electrode and OLED, respectively, and C is a typical value [14], Equation (6) produces the solid line shown in Figure 3 with a variable parameter of $A = 2.88 \times 10^6$ and $6.35 \times 10^5 \text{ count C}^{-1}$ for the ITO/TPD/Alq₃/Al and ITO/CoPc/Alq₃/Al devices, respectively. Equations (5) and (6) clearly indicate that ΔI also depends

on the time of the reverse-bias application t . Figure 5 depicts the t^{-1} (i.e., $2f$) dependence of ΔI derived from Figure 2 together with the values calculated using the parameter sets in Figure 3. Clearly, they are not consistent. This might be because A is not a common constant for t but a function of t . At this time, we cannot evaluate $A(t)$.

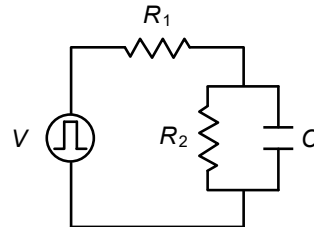


Figure 4. Equivalent circuit based on a model in which the OLED acts as a capacitor during the reverse bias. Here, V is the absolute value of the applied voltage, R_1 is the internal resistance, R_2 is the resistance of the OLED, and C is capacitance.

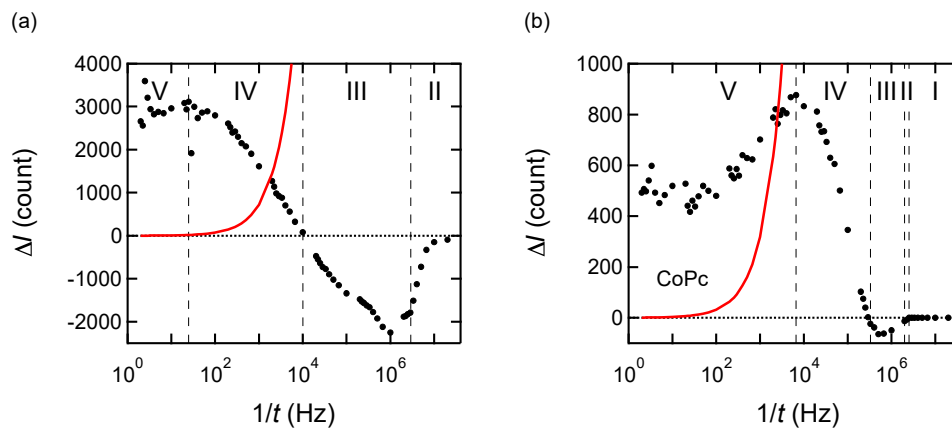


Figure 5. ΔI versus the reciprocal of t , i.e., $2f$, for the ITO/TPD/Alq₃/Al device (a) and ITO/CoPc/Alq₃/Al device (b). The solid line is calculated by Equation (6) with the parameter sets used in Figure 3. To interpret the t dependence of ΔI , we divided t into five regions, I, II, III, IV, and V.

To understand the mechanism of the reverse-bias emission enhancement, we consider the vacuum level shift (Δ) at the organic/metal interface. When a reverse bias is applied to an OLED and it acts as a capacitor, the interfacial dipole at the organic/ITO interface with negative (positive) Δ decreases (increases), while that at the organic/Al interface with negative (positive) Δ increases (decreases), because of the accumulation of negative and positive charges at the organic/ITO and organic/Al interfaces, respectively. In any case, whether Δ at the organic/metal interfaces is negative or positive, this situation causes Δ at the organic/ITO interface to shift positively and Δ at the organic/Al interface to shift negatively. Therefore, the vacuum level shifts at the organic/metal interfaces were modulated to shift both the HOMO of a hole injection material and the LUMO of an electron injection material close to the Fermi levels of the ITO and Al electrodes, respectively, leading to a decrease in both the hole injection barrier at the organic/ITO interface and the electron injection barrier at the organic/Al interface. Consequently, we believe that both the hole and electron injections occur easily under forward bias after reverse bias has been applied, resulting in an increase of the number of carriers that can arrive at the organic/organic interface compared to ordinary DC or alternating zero-forward bias.

Based on this model, we can interpret the tendency of ΔI to depend on t by dividing Figure 5 into five regions, I, II, III, IV and V, according to t .

In region I, no emission was observed for both the alternating zero-forward and reverse-forward biases. In this study, only the ITO/CoPc/Alq₃/Al device has a region I, meaning that no carriers can arrive at the CoPc/Alq₃ interface under the high frequency bias.

In region II, emission was only observed under the alternating zero-forward bias. The carriers can arrive at the organic/organic interface during the forward-bias phase of the alternating zero-forward bias. In contrast, under the alternating reverse-forward bias, the carriers are consumed to cancel the accumulated charges. As a result, because few residual carriers occur during the forward bias, the emission under the alternating reverse-forward bias is not observed, leading to a negative value of ΔI in this region.

In region III, emission was also observed under alternating reverse-forward bias. Above t of region II, residual carriers exist that can arrive at the organic/organic interface during the forward-bias phase of the alternating reverse-forward bias. However, the emission intensity under the alternating reverse-forward bias is smaller than that under the alternating zero-forward bias because most carriers are also consumed to cancel the accumulated charges. Therefore, ΔI is still negative, even though it increases as t increases above 1.0×10^{-6} and 2.0×10^{-6} s (corresponding to the frequency below 5.0×10^5 and 2.5×10^5 Hz) for the ITO/TPD/Alq₃/Al and ITO/CoPc/Alq₃/Al devices, respectively.

In region IV, ΔI is positive and increases with increasing t . In this region, the number of carriers that can arrive at the organic/organic interface during the forward-bias phase of the alternating reverse-forward bias exceeds that of the alternating zero-forward bias because of the injection-barrier suppression by the modulation of the vacuum level shift Δ .

In region V, where t is above region IV, ΔI decreases with increasing t . Because the suppression of the carrier injection barrier caused by the reverse-forward bias works only until the modulation of Δ induced by the accumulated charges generated under the reverse bias is canceled by the forward bias, the number of the carriers that can arrive at the organic/organic interface during the forward bias after the cancelation is similar to that in the zero-forward bias. Therefore, during large t , the device cannot obtain the entire benefit from the reverse bias in one pulse, causing ΔI to decrease. For our device, the most efficient condition for the ITO/TPD/Alq₃/Al and ITO/CoPc/Alq₃/Al devices is the reverse-forward alternating bias at a frequency of 1.2×10^1 and 3.3×10^3 Hz, respectively, where the emission intensity is 20% and 40% larger than that under the zero-forward alternating bias.

The frequency region where ΔI increases is consistent with that of ordinary interfacial polarization [15], suggesting that the proposed model and mechanism for emission enhancement are appropriate. Furthermore, very recently, charge accumulation at the Alq₃/cathode interface during the reverse-bias application has been reported [16], which supports our model. Here, we would like to emphasize that our model, in which accumulated charges at the organic/metal interfaces during the reverse bias enhance emission intensity, does not exclude the model in [7], in which accumulated excess charges at the organic/organic interfaces under the zero-forward bias suppress emission intensity; both types of accumulated charges should contribute to the device properties.

4. Conclusions

In conclusion, under the application of alternating reverse and forward rectangular biases, it was revealed that the emission properties of OLEDs depend on both the frequency and applied voltage of the reverse bias. The emission intensity under the alternating reverse-forward bias becomes larger than that under the alternating zero-forward bias as the level of reverse-bias voltage increases or as the frequency decreases. To interpret the change in the emission intensity (ΔI), we proposed a model in which the OLED works as a capacitor under reverse bias, and the accumulated charges at the organic/metal interfaces induce an enhancement of emission under the alternating reverse-forward bias. Based on the equivalent circuit of the model, an equation expressing the correlation between ΔI and the accumulated charges generated during reverse bias was derived. Experimental results for the applied reverse-bias voltage dependence of ΔI were adequately reproduced by the equation. Furthermore, our model can rationalize the emission enhancement, by considering

that the accumulated charges at the organic/metal interfaces modulate the vacuum level shifts at the organic/metal interfaces to reduce both the hole injection barrier at the organic/ITO interface and the electron injection barrier at the organic/Al interface under forward bias.

The model proposed in this study might be applicable to any OLED, suggesting that the application of a rectangular alternating reverse-forward bias is a fruitful method for tuning the light emission efficiency of OLEDs, and there is a fair possibility of obtaining higher device performances than under the ordinary DC bias.

Acknowledgments: This study was supported in part by Grant-in-Aid for Scientific Research (C) (No. 25410097 and No. 16K05752) from the Japan Society for the Promotion of Science.

Author Contributions: S.N. and M.M. conceived and designed the experiments; S.N. performed the experiments; S.N. and M.M. analyzed the data; M.M. wrote the paper.

Conflicts of Interest: The authors declare no conflict of interest.

References

1. Pope, M.; Kallmann, H.P.; Magnante, P. Electroluminescence in Organic Crystals. *J. Chem. Phys.* **1963**, *38*, 2042–2043. [[CrossRef](#)]
2. Tang, C.W.; VanSlyke, S.A. Organic electroluminescent diodes. *Appl. Phys. Lett.* **1987**, *51*, 913–915. [[CrossRef](#)]
3. Ishii, H.; Sugiyama, K.; Ito, E.; Seki, K. Energy level alignment and interfacial electronic structures at organic/metal and organic/organic interfaces. *Adv. Mater.* **1999**, *11*, 605–625. [[CrossRef](#)]
4. Ishii, H.; Oji, H.; Ito, E.; Hayashi, N.; Yoshimura, D.; Seki, K. Energy level alignment and band bending at model interfaces of organic electroluminescent devices. *J. Lumin.* **2000**, *87–89*, 61–65. [[CrossRef](#)]
5. Taguchi, D.; Weis, M.; Manaka, T.; Iwamoto, M. Probing of carrier behavior in organic electroluminescent diode using electric field induced optical second-harmonic generation measurement. *Appl. Phys. Lett.* **2009**, *95*, 263310. [[CrossRef](#)]
6. Taguchi, D.; Inoue, S.; Zhang, L.; Li, J.; Weis, M.; Manaka, T.; Iwamoto, M. Analysis of organic light-emitting diode as a Maxwell-Wagner effect element by time-resolved optical second harmonic generation measurement. *J. Phys. Chem. Lett.* **2010**, *1*, 803–807. [[CrossRef](#)]
7. Sadakata, A.; Taguchi, D.; Yamamoto, T.; Furusawa, M.; Manaka, T.; Iwamoto, M. Analyzing two electroluminescence mode of indium tin oxide/ α -NPD/Alq₃/Al diodes by using large alternating current square voltages. *J. Appl. Phys.* **2011**, *110*, 103707. [[CrossRef](#)]
8. Sadakata, A.; Osada, K.; Taguchi, D.; Manaka, T.; Iwamoto, M. Probing space charge effect on electroluminescence of indium tin oxide (ITO)/N,N'-di-[(1-naphthyl)-N,N'-diphenyl]-(1,1'-biphenyl)-4,4'-diamine (α -NPD)/tris(8-hydroxy-quinolinato) aluminum (III) (Alq₃)/Al diodes by time-resolved electric-field-induced optical second-harmonic generation measurement. *Thin Solid Films* **2014**, *554*, 110–113. [[CrossRef](#)]
9. Zou, D.; Yahiro, M.; Tsutsui, T. Study on the degradation mechanism of organic light-emitting diodes (OLEDs). *Synth. Met.* **1997**, *91*, 191–193. [[CrossRef](#)]
10. Zou, D.; Yahiro, M.; Tsutsui, T. Improvement of current-voltage characteristics in organic light emitting diodes by application of reversed-bias voltage. *Jpn. J. Appl. Phys.* **1998**, *37*, L1406–L1408. [[CrossRef](#)]
11. Lever, A.B.P. The phthalocyanines. *Advan. Inorg. Chem. Radiochem.* **1965**, *7*, 27–114. [[CrossRef](#)]
12. Zhu, L.; Tang, H.; Harima, Y.; Kunugi, Y.; Yamashita, K.; Ohshita, J.; Kunai, A. A relationship between driving voltage and the highest occupied molecular orbital level of hole-transporting metallophthalocyanine layer for organic electroluminescence devices. *Thin Solid Films* **2001**, *396*, 213–218. [[CrossRef](#)]
13. Brütting, W.; Berleb, S.; Mückl, A.G. Device physics of organic light-emitting diodes based on molecular materials. *Org. Electron.* **2001**, *2*, 1–36. [[CrossRef](#)]
14. Mo, B.; Zhang, X.; Liu, L.; Wang, H.; Xu, J.; Wang, H.; Wei, B. Bilayer-structure white organic light-emitting diode based on [Alq₃:rubrene] and the electron transporting characteristics investigation using impedance spectroscopy. *Opt. Laser Technol.* **2015**, *68*, 202–205. [[CrossRef](#)]

15. Van Krevelen, D.W.; Hoftyzer, P.J. *Properties of Polymers: Correlations with Chemical Structure*; Elsevier: New York, NY, USA, 1972; pp. 217–218.
16. Lee, J.-H.; Lin, B.-Y.; Shih, Y.-C.; Wang, L.; Chiu, T.-L.; Lin, C.-F. Increase of current density and luminescence in organic light-emitting diode with reverse bias driving. *Organ. Electron.* **2017**, *48*, 330–335. [[CrossRef](#)]



© 2017 by the authors. Licensee MDPI, Basel, Switzerland. This article is an open access article distributed under the terms and conditions of the Creative Commons Attribution (CC BY) license (<http://creativecommons.org/licenses/by/4.0/>).